

Reversibly Photoswitchable High-Aspect Ratio Surfaces

Gissela Constante, Indra Apsite, Dennis Schönfeld, Thorsten Pretsch, and Leonid Ionov*

Herein, the fabrication of light-sensitive high-aspect ratio surfaces with switchable topography using melt-electrowriting of shape-memory polymers and deposition of light-to-heat converting black ink on it by dip coating is reported on. The lamellae exposed to low temperatures are hard and cannot be deformed by water droplets. The temperature reached upon illumination of surfaces is close to the melting point of the soft segment of the polyurethane that leads to softening of the polymer. Due to this, it is possible to locally deform and recover the light-softened surface structures by water droplets deposited on lamellae. The deformed state can be fixed by cooling down resulting in the crystallization of the polymer. Thus, the reversibility of local deformation can be achieved. Finally, the application of the developed approach and materials for the fabrication of smart light-controlled valves is demonstrated, which can be used for the controlled mixing of fluids in microfluidic devices.

or by applying any other stimuli such as light or temperature leading to bending, stretching, or compressing of micro- and nanostructures.^[8]

The materials that can switch one or more properties in response to applied stimuli are known as “smart” materials. Smart materials convert one form of energy like thermal, electrical, chemical, or mechanical into another form.^[9] Two-way transformation is usually achieved using hydrogels, electroactive polymers, and liquid crystalline elastomers.^[10] Traditional shape-memory polymers (SMPs) allow only one-way shape transformation (relaxation from temporary shape to permanent one). The transformation to a temporary shape is usually achieved manually. SMPs can also be used for the design of surfaces with switchable topogra-

1. Introduction

Flat (2D), curved (3D), and hierarchical (3D) surfaces with dynamic topography attract rising interest due to their growing potential in medicine,^[1] biotechnology,^[2] electronics,^[3] robotics,^[4] and design of actuators,^[5] among others. The reshaping of the 2D surfaces or transformation of 3D surfaces in other 3D surfaces is usually triggered by either a physical or chemical stimulus, which can affect surfaces in two different ways: by changing the topography and/or by changing the chemical composition of the surface.^[6] The change in the topography can be, for example, achieved by the action of a mechanical force (physical stimuli)^[7]


phy,^[11] although their manual deformation to temporary states is unavoidable.^[12]

The shape-changing of SMPs is driven by the release of inner stress triggered by external stimuli like an increase in temperature.^[13] Although thermoresponsive SMPs have a high recovery ratio, up to 100%, their local actuation is challenging because of the difficulty of local heating. The light as a signal can solve these problems of local triggering because local illumination is very straightforward. Moreover, light-responsive materials allowed remote activation, temporal control, and rapid switching.^[14] Light-responsive materials actuate in different modes: 1) the first one by changing the conformational structure of photochromic groups (photochemically), for example, spiropyrans and azobenzenes;^[15] 2) the second one by elevating the excitation level of the photochromic groups;^[16] and 3) the third one by the transformation of light energy into heat known as a photothermal effect.^[15,17] Photothermal effect allows local heating of, for example, polymers above their glass transition and/or melting temperature and, as follows, allows their local softening.^[18] The typical photothermal materials, which absorb light and convert it into heat,^[19] are carbon nanomaterials, gold nanomaterials, indocyanine green, and metallic sulfides/oxides.^[20] The use of photothermal effects is in many cases more preferential because it allows separate tuning of properties of the thermoresponsive matrix and light-sensitive (photothermal) agents. An example of the application of the photothermal effect was observed in the control of light-responsive hydrogel valves used in microfluidic devices.^[21] Another interesting example of a photothermal-responsive surface is presented by Jiao et al.^[22] In their investigation, an anisotropic grooved surface composed of graphene and polyvinylidene coated with paraffin was created to control the droplet sliding. By the photothermal stimuli, the topographical surface is modified to manipulate the water drop,

G. Constante, I. Apsite, L. Ionov
Faculty of Engineering Sciences
University of Bayreuth
Ludwig Thoma Str. 36A, 95447 Bayreuth, Germany
E-mail: leonid.ionov@uni-bayreuth.de

D. Schönfeld, T. Pretsch
Shape Memory Polymers Group
Synthesis and Polymer Technology
Fraunhofer Institute for Applied Polymer Research IAP
Geiselbergstr. 69, 14476 Potsdam, Germany

L. Ionov
Bavarian Polymer Institute
University of Bayreuth
95447 Bayreuth, Germany

 The ORCID identification number(s) for the author(s) of this article can be found under <https://doi.org/10.1002/ssstr.202300040>.

© 2023 The Authors. Small Structures published by Wiley-VCH GmbH. This is an open access article under the terms of the Creative Commons Attribution License, which permits use, distribution and reproduction in any medium, provided the original work is properly cited.

DOI: 10.1002/ssstr.202300040

either pinning or sliding, effect used for the fabrication of anti-icing surfaces.^[22]

In our previous work, we demonstrate an approach for the fabrication of surfaces with switchable high-aspect ratio lamellae based on SMPs using melt-electrowriting (MEW).^[23] The mechanical properties of the lamellae can be switched between soft and hard states. The high-aspect ratio lamellae demonstrated possibilities to switch their shape by surface tension of the water and temperature, and manual deformation was not required. The temperature as a signal, used in our previous work,^[23] can hardly be applied locally to achieve targeted switching of mechanical and wetting properties of surfaces. Using light as a signal presents more benefits. In this article, we have taken a step forward in designing high-aspect ratio surfaces with switchable topography and made them light-sensitive, which we expect should allow local manipulation with topography and wetting. The dip coating as the selected method for converting the lamellar surface into a photoresponsive is advantageous because it is simple, efficient, and inexpensive, and as the particles are not

embedded into the molten polymer, the rheological properties and printing conditions are not affected.

2. Results and Discussion

The high-aspect ratio light-sensitive surfaces were fabricated using a two-step approach (Figure 1). First, lamellae of shape-memory poly(1,4-butylene adipate)-based polyurethane (TPU PBA-75) copolymer were deposited on a glass substrate using MEW (Figure 1a). In the second step, a layer of black light-absorbing ink was deposited on the top of the lamellae (Figure 1b). The use of two-step approach has essential advantages over the approach of light-absorbing material, which is usually carbon, iron oxide, or similar black particles, is mixed into the polymer and the polymer-particle blend is then deposited. In fact, it is known that particles are able to substantially change the rheological behavior of polymer melts, in particular when the particles tend to aggregate. The aggregated particles render

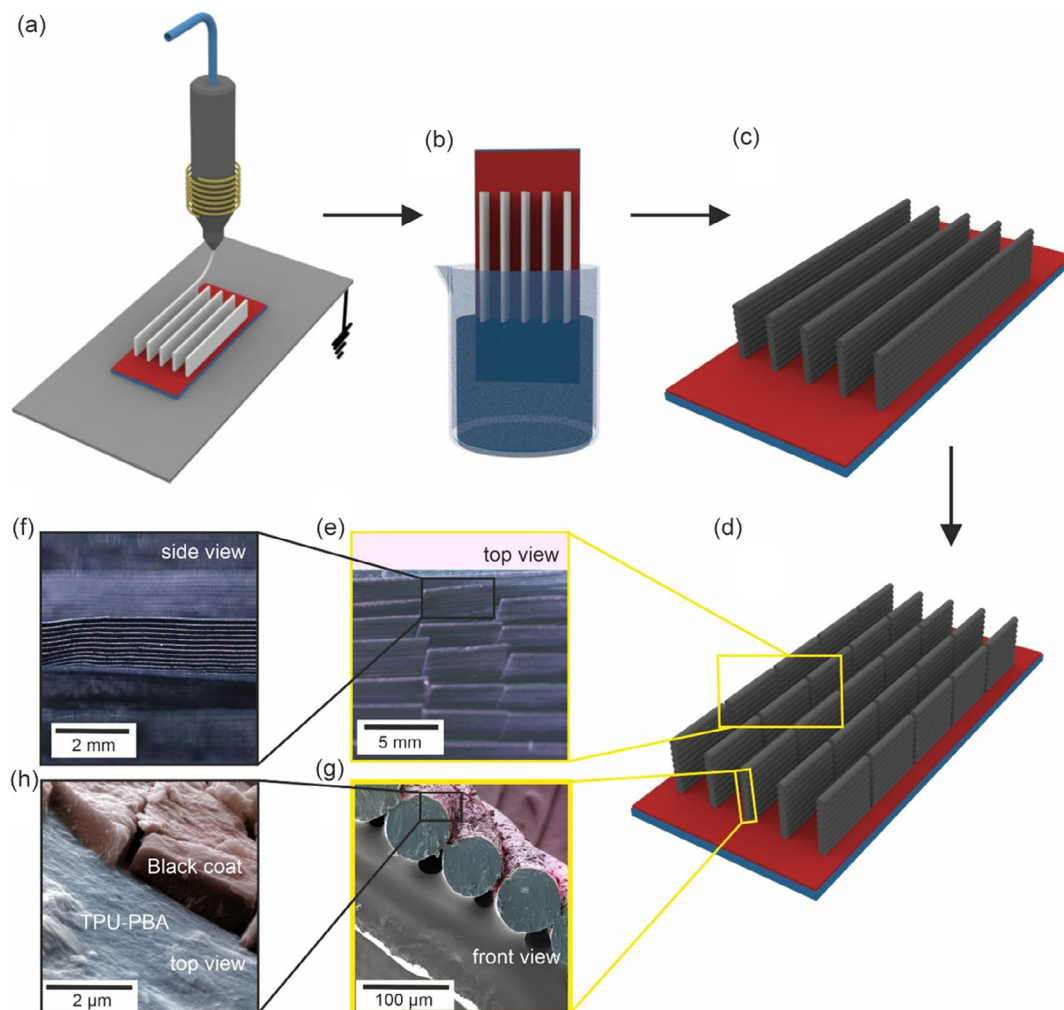


Figure 1. Scheme of fabrication of photosensitive structured surfaces with high-aspect ratio lamellae: a) fabrication of TPU-PBA lamellae using MEW; b) deposition of light-absorbing material on the lamellae using dip coating to form light-sensitive surfaces; c,d) the lamellae may be cut to reduce their length and form short flaps to increase the amplitude of actuation; e,f) optical imaging made with a macrocamera, and g,h) SEM of the surface of the black-coated lamella (pink color: black coating, blue color: polymeric fiber).

the polymer's flow behavior with flow threshold points.^[24] Such blends show elastic behavior over a very broad time-scale range and nearly do not flow when small stress is applied. The blends start to flow when the stress above a threshold value is applied.^[24] Such kind of behavior makes the control of the flow behavior of polymers difficult. Therefore, in order to avoid these difficulties, we used a two-step approach—deposited polymer first and light-absorbing material next. Another advantage of this approach is that amount of light-absorbing material can be easily controlled in two ways: by its concentration in dispersion/solution and by varying the number of layers, which are deposited. On the contrary, the use of a one-step approach will require making new blends each time when the amount of light-absorbing material shall be varied. Thus, the main advantages of the use of a two-step fabrication approach are flexibility from point of view of fabrication of a variety of structures with different compositions and properties.

We have used poly(1,4-butylene adipate)-based polyurethane. The thermoresponsive polyurethane had a hard segment formed by the reaction between 4,4'-diphenylmethane diisocyanate (MDI) and 1,4-butanediol (BD). The soft segment was composed of poly(1,4-butylene adipate) (PBA). The soft segment possesses a melting peak temperature of around 40 °C and a crystallization onset temperature of 5 °C when applying a heating/cooling rate of 5 °C min⁻¹ (Figure S1a, Supporting Information). Cold crystallization in second heating cycle disappears at lower scan rate because conditions are closer to equilibrium and chains have enough time to crystallization upon cooling that is evidenced by higher crystallization enthalpy in cooling cycle (Figure S1a, b, Supporting Information).

The mechanical properties of the polymer showed that the material can be in two states: hard and soft depending on the temperature. The elastic modulus in the hard state is 55 MPa approximately and in the soft state 8 MPa.^[23] The low melting point of the mobile phase of poly(ester urethane) (PEU) can be easily attainable after few seconds of light exposure. As well, from the point of view of the mechanical properties, the PEU lamellar construct can be deformed by small forces as in the addition of water drop, eliminating the need of manual deformation.

The thickness of lamellae is determined by conditions of MEW ($V = 3$ kV, 200 μm of nozzle diameter, at 215 °C temperature and 2 mm distance from the electrified collector). The viscosity of the polymer decreased at a temperature over 200 °C as measured in the frequency sweep at a constant strain (5%) (Figure S3, Supporting Information) and by rotational rheology (Figure S4, Supporting Information) which shows the flowability of the polymer at 215 °C. The storage and loss moduli curves showed that the polymer starts to flow at temperatures higher than 180 °C as observed in Figure S2, Supporting Information. For the dip coating solution, we used commercial black ink as light-absorbing material—Edding T100 (Ahrensburg, Germany). The reasons for the selection of this material are the following: 1) it has a high extinction coefficient in a whole range of visible light (the material is very black even if the thickness of the layer is small); 2) it forms stable dispersion. The measured thickness of the coating was $0.9 \pm 0.1 \mu\text{m}$ (Figure 1g,h) as it was measured using scanning electronic microscopy (SEM). This behavior is, however, expected in all kinds of inorganic granular materials—contact between particles is weak and breaks at low strain. After 5 and 10 cycles of deformation, the samples were analyzed by SEM (Figure S5, Supporting Information). It was observed that the black coating was stable; nevertheless, after 10 cycles of deformation, the coating formed few cracks on the surface of the polymeric lamella.

Next, we investigated the mechanical properties of coated lamellae to explain the effect of light-absorbing coating and light stimulation. First, cyclic extensional strain testing was performed to elucidate the properties of materials at relatively large deformation up to $\epsilon = 25\%$ (Figure 2a). Young's modulus of the uncoated ("white") lamella was measured to be 49 ± 9 MPa. Exposure to light results in the decrease of the modulus down to 25 ± 3 MPa, which is explained by the increase of temperature of the material due to the photothermal effect and its softening due to melting of poly(1,4-butylene adipate) block—even white materials are able to absorb light which results in their softening. Young's modulus for the coated ("black") lamella with and without light exposure was 42 ± 2 and 6 ± 1 MPa, respectively (Figure 2a). The drop in Young's modulus is due to the melting

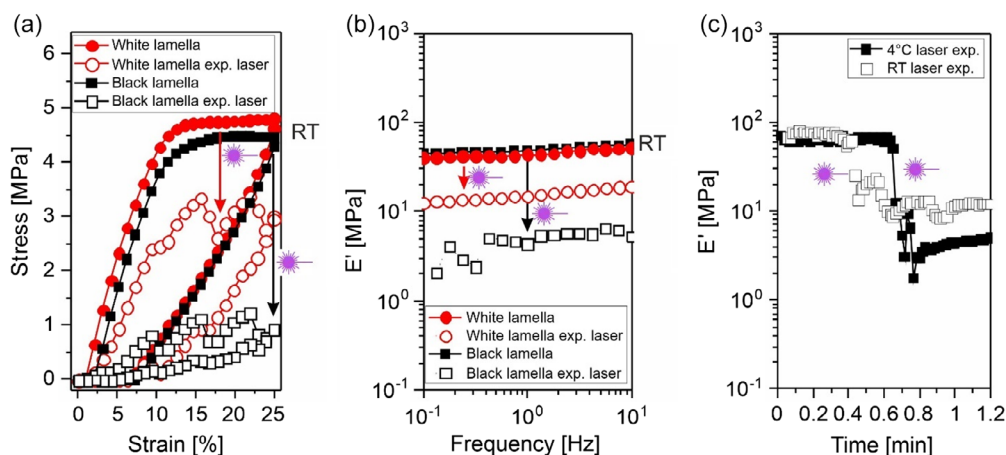


Figure 2. Mechanical characterization of the lamellae noncoated (white lamella) and coated with black ink (black lamella): a) a cyclic strain dynamic mechanical characterization ($\epsilon_{\text{max}} = 25\%$) exposed and not exposed to light; b) frequency sweep characterization of lamella exposed and not exposed to light and coated and not coated with black ink; c) storage moduli of the black lamella when exposed to 4 °C and kept at RT.

of the soft segment of the polymer. The obtained values of Young's modulus of nonexposed lamellae with and without black coating allow a conclusion that the black coating does not affect Young's modulus of the lamella—contribution of thin and brittle particle layer to mechanical properties is negligible. On the other hand, black coating significantly improved the light sensitivity of polymer lamellae and allows manipulation of its mechanical properties by light.

An extensional frequency sweep was performed to characterize the mechanical properties of the lamellae at different time scales (Figure 2b). It was found that storage modulus dominates over loss modulus for the coated lamellae, which were exposed to light (Figure S6, Supporting Information). Therefore, the values of loss moduli are not shown. It was found that the storage modulus decreases tenfold from 49.1 to 4.7 MPa when the coated lamella was exposed to light (Table S1, Supporting Information). The storage modulus of uncoated lamellae decreases from 44.6 to 15.5 MPa which is 3 times lower than that in the case of coated lamellae. As mentioned above, this is explained by the inherent heat produced by light. Nevertheless, the storage modulus was still higher than that obtained when the material was exposed to 40 °C (8 MPa).^[23] We did not observe any frequency dependence of storage modulus for coated and uncoated samples, which were exposed and not exposed to light. This means that softening of the polymer does not result in the appearance of a relaxation process on the investigated time scale.

In the third experiment, we studied the rate of softening of the polymer upon exposure to light (Figure 2c). We tested two kinds of lamellae: one, which was kept at room temperature (RT), and one, which was exposed to 4 °C to induce stronger crystallization. It was found that illumination with light resulted in the drop of Young's modulus on a time scale of a few seconds independent of how the sample was treated. This observation shows that softening of lamellae is a fast process. The mechanical tests clearly showed that the mechanical properties of coated lamellae can be manipulated by light and that softening of the polymer is very quick.

We studied the photothermal shape-memory behavior (deformation, fixation, and recovery) of the lamellae (Figure 3). First, the crystallized lamella was stretched by applying stress $\sigma = 5$ MPa which resulted in their elongation by $\epsilon = 3\%$. Then, the stressed lamella was exposed to light which resulted in its deformation by $\epsilon = 80\%$. The whole stretching process took

≈ 200 s that is because illumination was local and heating of the whole lamella takes a certain time. The shape fixation was performed by pouring liquid nitrogen vapor onto the sample in a stretched state. After that, the stress was released ($\sigma = 0$ MPa), and the strain was reduced to 73% due to the partial relaxation of the polymer chains. Nearly full shape recovery was achieved upon light exposure for 3 min. The final strain of the recovered sample was 3%. This experiment showed the possibility of photothermal actuation and thermal fixation of coated lamellae.

We studied the deformation of the coated lamella and flaps (5 mm long parts of lamella obtained by cutting) (Figure 4) by water droplet before and after illumination with light to investigate the interplay between surface tension and elastic forces. The nonilluminated lamella/flap could not be deformed by both advancing and receding water droplets. The lamella/flap was then exposed to light for 5 min to make it soft (Figure 4c,d), and then the surface temperature was set at 20 °C. The water droplet was deposited between lamellae/flaps (advancing droplet) which caused their deformation in the direction opposite to each other. Afterward, the droplet was soaked back (receding droplet) into the pipet to reduce its volume. Surface tension forces forced lamellae to bend toward each other. These findings show that the short flap experienced greater deformation (3.13 ± 0.7 mm) when exposed to light and advancing volume of water (Figure 4e). However, the difference between deformation of the continuous lamella and that of the short flap, when both were exposed to 4 °C before the deformation (which resulted in hard mechanical memory) or when they were exposed to light (resulting in soft mechanical memory), was found to be not significant. We also estimated the degree of deformation of the short flaps after the water volume was receded. Results showed that the maximum deformation of the short flaps that were exposed to light is 1.05 ± 0.2 mm. These findings confirm that lamellae can indeed be deformed at RT after exposure to light, and that once the stress is eliminated, the lamellae can recover their original position. This experiment showed that the sensitivity of coated lamellae to surface tension forces generated by water droplets can be switched by light.

The recovery of lamellae depends on their length. In order to investigate this phenomenon, we manually deformed heated long lamellae and then cooled them down to fix them in a temporary state. The recovery was induced by exposing lamellae to light. The recovery was measured in two areas of the surface: in

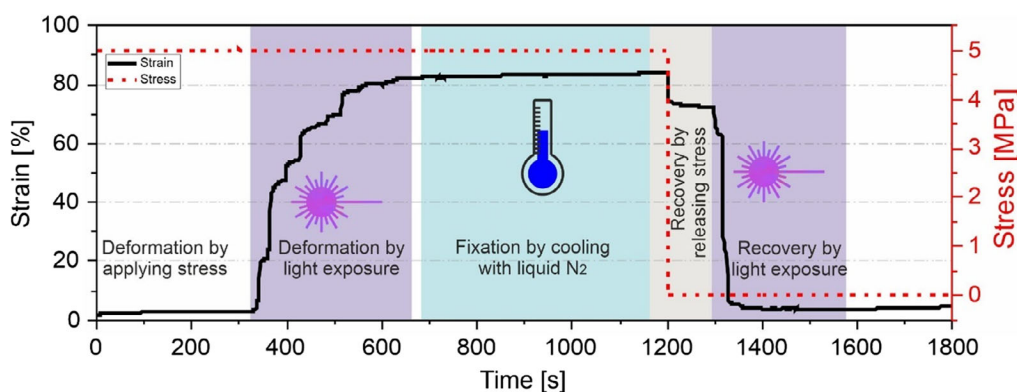


Figure 3. Photothermal shape-memory behavior of the black lamellae measured in dynamic mechanical analyzer at a constant stress ($\sigma = 5$ MPa) during deformation and $\sigma = 0$ MPa for recovery.

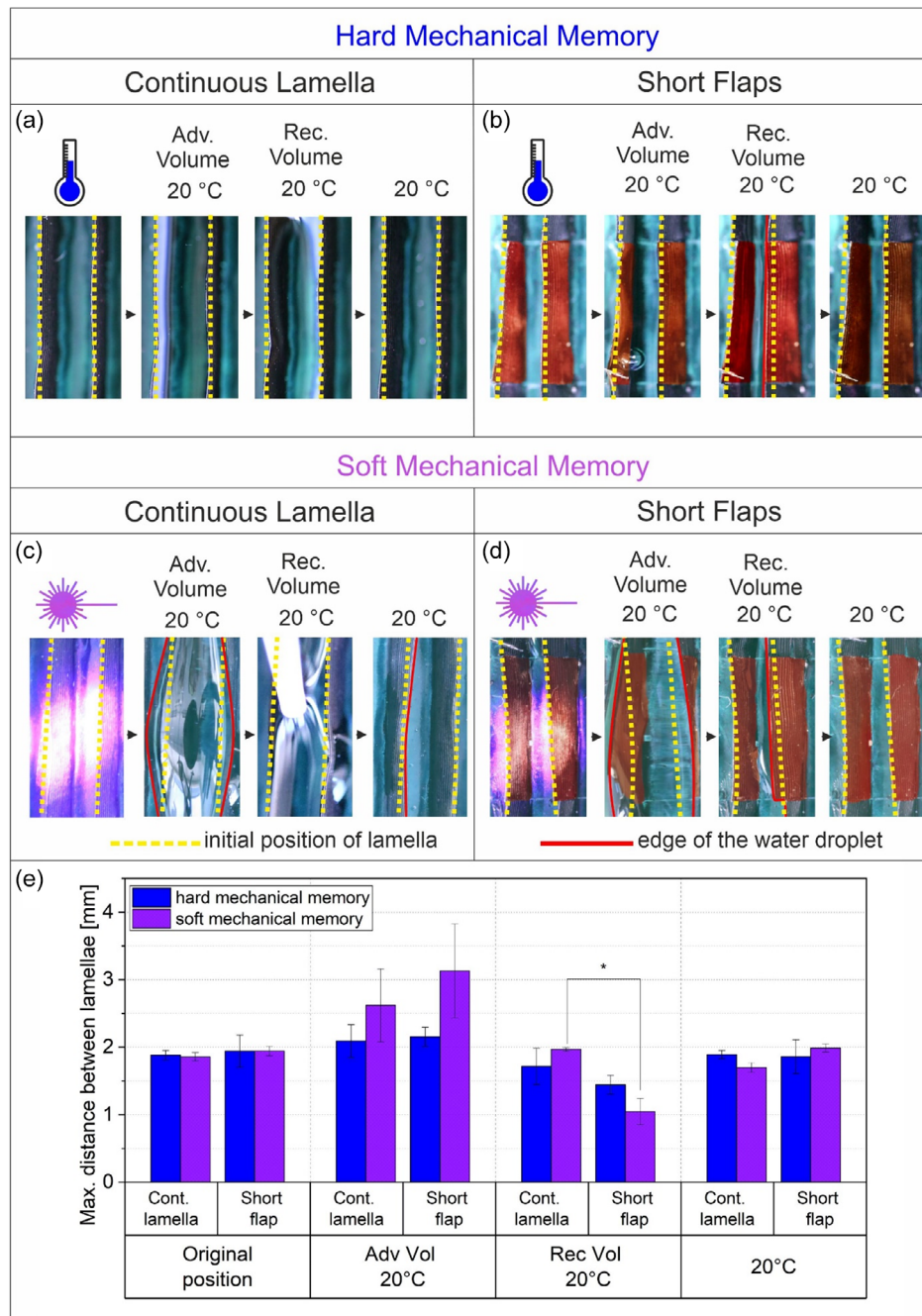


Figure 4. Deformation of the lamellae (left column a,c) and short flaps (right column b,d) exposed to 4 °C (hard state, upper panel (a) and (b)) and illuminated before deformation (soft state, lower panel, (c) and (d)). Dashed yellow line—lamella in the initial state, red line—edge of the water droplet after deformation. The short flaps were colored in red to facilitate the visualization. (e) Maximum distance measured between the lamellae. (* at the 0.05 level, there is a significant difference in the means) (ANOVA and Tukey test at $p = 0.05$; $n = 2$).

the center of the lamella and at the edges (Figure 5). It was observed that the recovery of the central part of lamella occurred within 600 s of light exposure was 21%, while the recovery of the edges reached 28% in 10 s of exposure. The reason for this difference is the inhomogeneous heating of the sample surface by light (Figure 5d). Indeed, complete recovery is only possible when the whole lamella is heated—hard nonilluminated part

of lamellae oppose deformation. Heating of a fraction of lamella does not result in the recovery of even heated areas—the structure behaves as a beam with two fixed ends. The edge of the lamella is, however, “fixed” at one of its ends, which is the long lamella. As result, its recovery is large. This observation indicates that a large recovery can be achieved when the whole lamella is illuminated which can be realized by the use of a large and

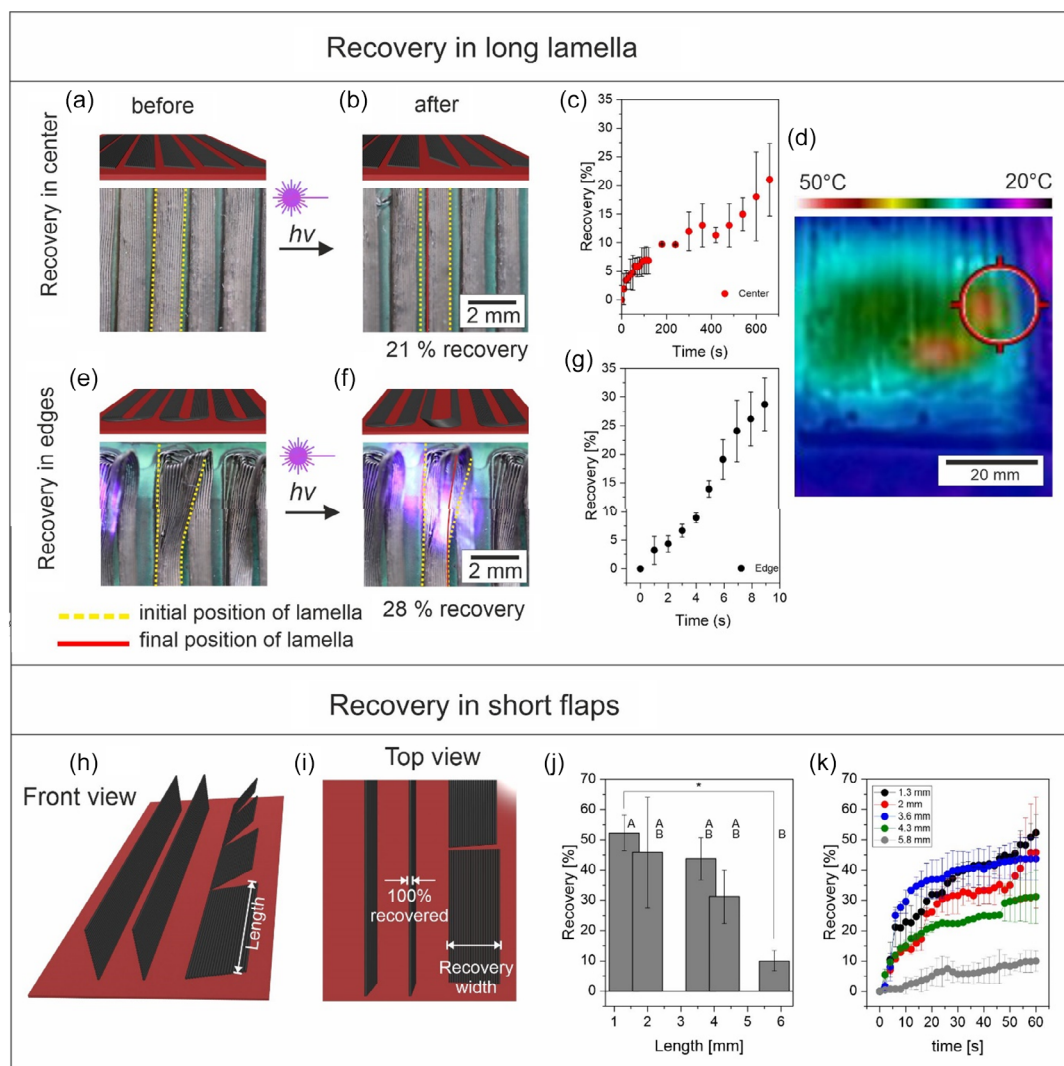


Figure 5. Studies of the efficiency of recovery of lamellae depending on their length: a–c) central part of lamellae is illuminated; e–g) edges of the lamella are illuminated; d) photothermal photography of the exposed areas to light. Yellow dashed line—initial position of the lamella, red line—final position of lamella after restoring; h,i) front and top view of the lamellae flaps at different length; j) achieved recovery after 60 s of light exposure while varying the length of the flap; and k) the recovery curve for flaps of different length.

sufficiently powerful laser beam or by the use of short lamellae. Moreover, in order to determine the efficiency of recovery of the short flaps, we cut the lamellae in different lengths: 1.3, 2, 3.6, 4.3, and 5.8 mm, and measured the width of the flap (Figure 5i) at different times during light exposure (Figure 5k). A fast recovery of the flap was observed at small lengths. After 60 s of exposure, a maximum of 52% of recovery was observed for flaps of 1.3 mm. There is a statistical difference of the recovery percentage between the flaps of 1.3 and 5.8 mm length at a significance of 95% (Figure 5j).

As discussed in our previous article,^[23] it is evidenced that the surface tension ($F_s \approx \gamma \cdot dl$),^[25] elastic deformation ($\delta \approx F \cdot H^3 / EI$, where H is the height of lamella, I is the second moment of inertia $I = a \cdot dl^3 / 12$, a is the thickness of a lamella, and dl is its length), and gravity ($F_g \approx \rho \cdot g \cdot h \cdot b \cdot dl$, where h is the height of the droplet and S is the surface area) interact to deform the lamellae.

The deflection is $\delta \approx \frac{\gamma \cdot H^3}{E \cdot a \cdot dl^2}$ and it decreases with the length of flaps. Thus, not complete heating of lamellae by light is not the only reason for weaker deformation of long lamellae. The longer are the flaps, the weaker they deform.

Two previous experiments showed separately that surface tension forces can cause considerable deformation of lamellae, deformation/recovery depends on the length of lamellae, and recovery can be induced by light. Therefore, we investigated the possibilities to induce deformation/recovery of lamellae by a combination of surface tension forces and light (Figure 6). We fabricated lamellae and cut a flap with a length ≈ 5 mm, which was further actuated by water droplets and light. Water droplet was deposited between two flaps and the flaps were illuminated with light to soften them. The water droplet was either advanced or receded. We observed that water droplets deformed flaps upon their illumination with light. Afterward, the

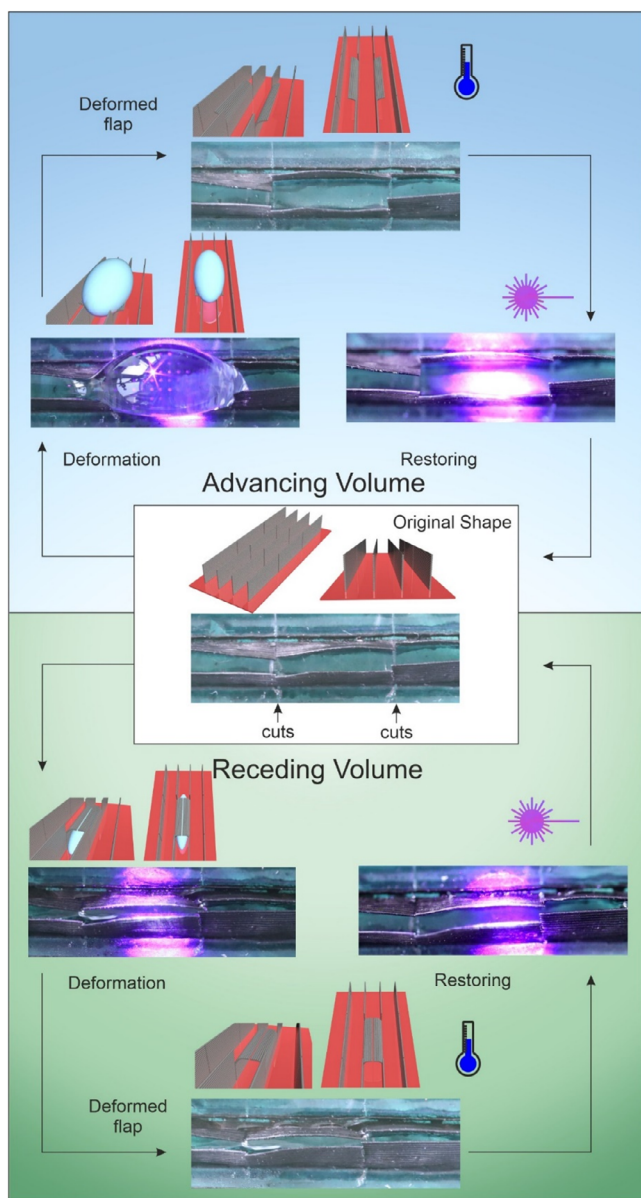


Figure 6. Deformation and recovery of the flaps made by light exposure by advancing volume droplet and receding volume water droplet.

temperature was reduced to 4 °C using the Peltier element, where the sample was placed, to store the temporary shape (deformed flap). The lamellae stayed in a temporary deformed state after the water droplet was removed. Illumination with light resulted in the recovery of deformed lamellae within 30–60 s. The recovery with light exposure was 5 times faster than the one achieved with thermal exposure in our previous investigation.^[23] The reason for this difference is most probably faster heating with light—lamellae get heated by light faster because they directly absorb light. In the case of thermal heating, the heat needs to diffuse through the sample. It is important that the illumination of flaps, which contact with water droplets, does not result in their softening and bending. Indeed, the maximum

temperature reached in the water environment can be up to 27–28 °C which is 12 °C lower than the minimum required to bend the structures (Figure S7, Supporting Information). Such a big difference in comparison to behavior in the air can be explained by the heat capacity of the water, which is 4182 J kg⁻¹ K, which is much higher than that of air, that is, 1005 J kg⁻¹ K (density of air is much lower than that of water).^[26]

Finally, we demonstrated the application of photothermally sensitive lamellae for the design of smart valves for microfluidic devices. We fabricated rectangular reservoirs for liquids. The walls of these reservoirs are formed by lamellae. The lamellae were cut with scissors to form flaps, which will act as valves. The main advantage of black-ink-coated flaps is the possibility of their individual control—they can be actuated independently from each other. Unlike our previous article,^[23] where only recovery of the whole sample by heating was possible, here, each flap can soften individually which allows the design of smart light-controlled smart valves that can be used to control the mixing of liquids on a microscale.

An example of a such device with light-controlled valves is shown in **Figure 7**. Two valves (shown by red and yellow rectangles) were softened by light exposure to allow advancing water. When both valves remained in a closed state (no bending), the liquid, colored in red, did not flow out of the groove (Figure 7b). Illumination with light softens the lamellae that allow their bending by increasing the volume of the water in the channels (Figure 7c,d). The mixing of both fluids depended on the flow rate. It was possible to limit the mixing rate by an incomplete opening of the valve (e.g., using a half-opened valve) and by reducing the volume of liquids. After mixing, the temperature was rapidly dropped to 4 °C to fix the temporary shape. The recovery of the valves was made in the absence of the liquid because the forces exerted by the water droplet on the deformed flap (gravity, weight, capillarity force) restricted the recovery of the flap. Moreover, the temperature achieved during the photostimulation of the black lamella when it was in the contact with water is lower than the minimum required to get the soft state of the surface that is due to the higher heat conductivity of water discussed above (Figure S7, Supporting Information). The recovery time for each valve was different, possibly explained by the length of the valve. For the valve in a red rectangle, the time was 52 s, while for the valve in a yellow square took 84 s to recover.

3. Conclusion

This article reports the fabrication of light-sensitive structured surfaces with high-aspect ratio lamellae and lamellae flaps. The high-aspect ratio features were fabricated using MEW. The sensitivity to light was provided by using a combination of thermoresponsive SMP and its coating by black ink, which converts light into heat. The approach suggested in this study is a simple method involving dipping the lamellar surface into a black ink solution to stain the surface of the polymeric lamellae. Unlike incorporating black particles within the polymer, this method does not affect the degree of crystallinity of the material.

The lamellae exposed to low temperatures are hard and cannot be deformed by water droplets. The temperature reached upon exposure to light-coated polymer was close to the melting peak

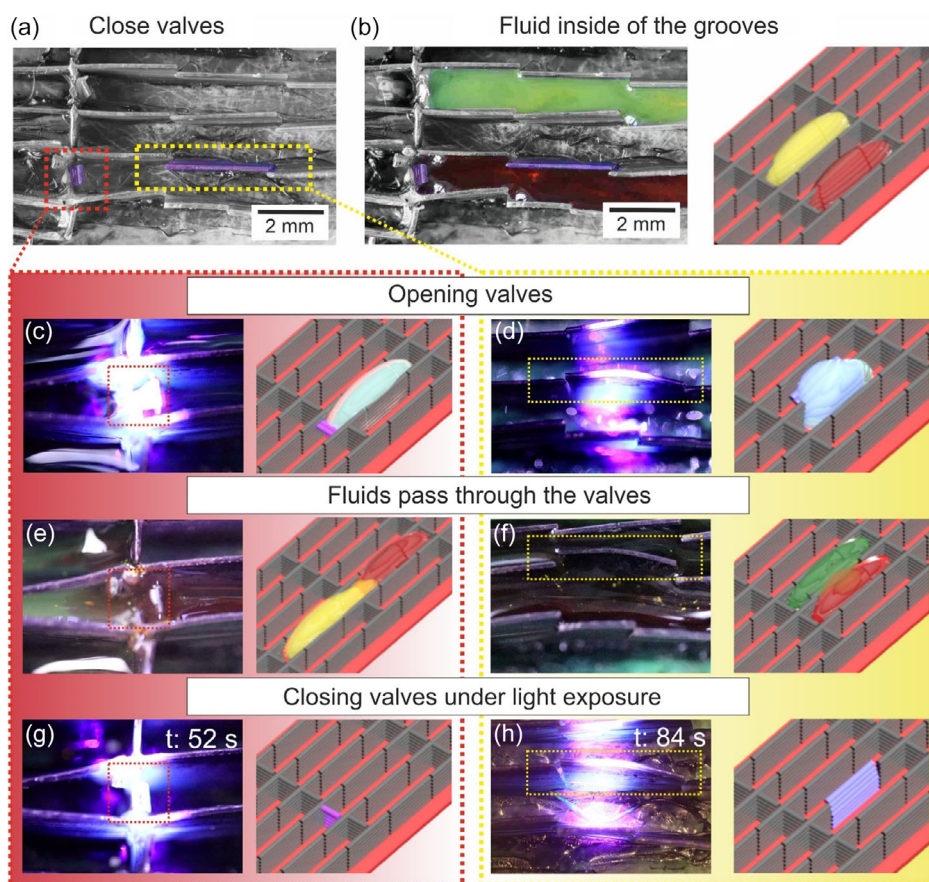


Figure 7. Use of multiple independently light-controlled smart valves for control of mixing of liquids: a) valves are closed and b) the liquid (colored in yellow and red) remained inside of the cavities formed by the flaps; c,d) by advancing volume of the water, the smart valves opened; and e,f) the fluids combined and circulated to other grooves. g,h) The recovery of the position of the flaps was conducted by photothermal effect; smart valves are highlighted in red and yellow squares.

temperature of the soft segment of the polyurethane which led to softening of the polymer. Due to this effect, it was possible to deform and recover the surface by water droplets deposited on lamellae. This soft state can be preserved even after exposition to light which allows deformation due to the soft mechanical memory shown by the surface. The deformed state can be fixed by cooling down resulting in the crystallization of the polymer. The deformation and recovery extent as well as rate depend on the length of lamellae—shorter lamellae flaps are deformed stronger, recovered complete, and do it faster than long ones that are also due to inhomogeneity of heating. Finally, we demonstrated the application of the developed approach and materials for the fabrication of smart light-controlled valves, which can be used for the controlled mixing of fluids in microfluidic devices. This brings a potential application in the creation of multiple smart valves that can act independently, opening and closing the passage for combining fluids and reactions.

4. Experimental Section

Materials: For the fabrication of the lamellar surface, a thermoresponsive polyester urethane (polybutylene adipate based) was required. For its

synthesis, poly(1,4-butylene adipate) (PBA) diol Desmophen 2505 was selected from Covestro Deutschland AG (Leverkusen, Germany) and 4,4'-diphenylmethane diisocyanate (MDI) was purchased from Fisher Scientific (Schwerte, Germany). 1,4-butanediol (BD), as well as a molecular sieve with a pore size of 4 Å, was obtained from Alfa Aesar (Kandel, Germany). Polylactide (PLA 4032D) was obtained from NatureWorks Ltd. (Minnetonka, MN, USA) and chloroform from Merck (Darmstadt, Germany). Black ink Edding T100 (Ahrensburg, Germany) was diluted with isopropanol from Merck (Darmstadt, Germany).

Synthesis of TPU: Poly(1,4-butylene)-based poly(ester urethane) (TPU PBA-75) was synthesized as previously described.^[23] Briefly, 0.037 mol of dried PBA-diol Desmophen 2505 reacted at 120 °C with 0.157 mol of MDI for 90 min. The isocyanate prepolymer reacted with 0.12 mol dried BD. The reaction stopped by pouring the melt onto a plate covered with a polytetrafluoroethylene film. Finally, TPU PBA-75 was cured in an oven at 80 °C for 120 min and ground into granules for further use.

Spin Coating of the Glass Slides: Glass slides of 26 mm × 76 mm were coated with 500 μL of a solution of PLA in chloroform (10 mg mL⁻¹) with a Spin Coater Ossila (UK). The rotational speed was set at 500 rpm for 10 s to ensure total coverage of the surface, and then it increased to 4000 rpm for 1 min.

Fabrication of the Surfaces: The lamellar surface was fabricated as previously described.^[23] Briefly, the MEW of TPU PBA-75 was made in a 3D Discovery printer Regen Hu (Villaz-St-Pierre, Switzerland). The conditions for MEW were set at 215 °C, 3 kV of voltage, pneumatic pressure at 0.1 MPa, the distance between collector and nozzle was 2 mm, and the

translation speed (F) was 100 mm s^{-1} . The extrusion was made with a metallic needle of $200 \mu\text{m}$ inner diameter. By stacking the fibers one upon each other, the lamellar surface was fabricated. To create the flap surface, the lamellae were cut transversally every 5 mm with a sharp razor blade. The distance between the lamellae was $1500 \mu\text{m}$, and the height was $1500 \mu\text{m}$.

Dip Coating: The lamellar surface was dip-coated in a solution of a commercial black ink Edding T100 (Germany) in isopropanol at 25% v/v. A dip coater Ossila (UK) was used. The samples were immersed for 10 s at 10 mm s^{-1} , followed by a withdrawal with a speed rate of 1 mm s^{-1} . The samples were dried in a vertical position.

SEM: The SEM photographs were made by using a scanning electron microscope Thermo Fischer Scientific Apreo 2 SEM (Germany). A lamella section was fixed on an SEM stub with the help of copper double-phase adhesive tape. The sample was sputtered with $\approx 1.3 \text{ nm}$ platinum to ensure conductivity using a Leica EM ACE600 (Wetzlar, Germany). The sputtering rate was set at 0.02 nm s^{-1} , with a current of 35 mA , under Argon 0.05 mbar .

Dynamical Mechanical Analysis: The mechanical properties of the material were measured in a Modular Compact Rheometer MCR 702 Multidrive from Anton Paar GmbH (Ostfildern, Germany). Mechanical properties measurement was done for the lamella when it was not black-coated and exposed and not exposed to light. A logarithmic frequency sweep from 100 to 0.1 Hz was done with constant extensional stress (σ) of 0.25 MPa . The white and black lamella were exposed to light for 3 s every 30 s to avoid the degradation of the material.

The extensional cyclic experiment was done in a linear ramp mode increasing the strain (ϵ) from 0.01% to 25% with an extension rate of $1\% \text{ min}^{-1}$.

To measure the elastic deformation and recovery of the black-coated lamellae, the rheological measurements were done in five steps: the first one was made at a constant stress of 5 MPa , and the strain was measured, which shows the deformation of the lamella for 300 s . In the second stage, the sample was exposed to light laser while keeping the stress at 5 MPa for 300 s . In this stage, the sample was exposed to light for 3 s every 30 s . The third stage was done by the fixation of the stretched lamella while pouring liquid nitrogen, and the stress was set at 5 MPa for 600 s . The fourth and fifth stages were the recovery of the sample by releasing the stress without and with light exposure, respectively.

For the light exposure, we used a violet laser diode module. The laser had a wavelength (λ) of 405 nm , class IIIb, with an elliptical beam with an adjustable focus. The distance between the sample and laser light was set at 10 cm for all the experiments.

Deformation Studies: The lamellae surface was cut into flaps of 5 mm in length. The deformation studies were made for the long lamella and the flaps. The deformation of the structure was made under the photothermal effect produced by light exposure while the water volume increased or decreased depending if it was advancing or receding volume. The shape-memory behavior of the structured topographical surface was studied by deforming the lamellae under light exposure. By advancing and receding the volume of a water drop, the lamellae were able to deform in the direction of the water flow. The sample was fixed by cooling it to $4 \text{ }^\circ\text{C}$. The recovery of the original state of the sample was accomplished by the photothermal effect provided by light exposure.

Statistical Analysis: The statistical analysis was made in Origin Lab software. Data were produced with two replicates. The analysis of variance (ANOVA) was performed at a significance of 95% ($p = 0.05$). Tukey test was used as comparison test at a $p = 0.05$.

Supporting Information

Supporting Information is available from the Wiley Online Library or from the author.

Acknowledgements

This work was supported by Deutsche Forschungsgemeinschaft (DFG) (grant no. IO 68/15-1). T.P. wishes to thank the European Regional

Development Fund for financing a large part of the laboratory equipment (project 85007031). Parts of this research were funded by Fraunhofer Excellence Cluster "Programmable Materials", grants number PSP elements 40-04068-2500-00007 and 40-03420-2500-00003. The authors would like to thank Prof. Scheibel for allowing the use of SEM device. The manuscript was written through contributions of all authors. All authors have given approval to the final version of the manuscript.

Conflict of Interest

The authors declare no conflict of interest.

Data Availability Statement

The data that support the findings of this study are available from the corresponding author upon reasonable request.

Keywords

light-responsive materials, shape-memory polymers, tunable materials, wetting

Received: January 31, 2023

Revised: May 17, 2023

Published online: June 6, 2023

- [1] a) A. Kirillova, L. Ionov, *J. Mater. Chem. B* **2019**, *7*, 1597; b) E. Gultepe, J. S. Randhawa, S. Kadam, S. Yamanaka, F. M. Selaru, E. J. Shin, A. N. Kalloo, D. H. Gracias, *Adv. Mater.* **2013**, *25*, 514.
- [2] a) A. Kirillova, R. Maxson, G. Stoychev, C. T. Gomillion, L. Ionov, *Adv. Mater.* **2017**, *29*, 1703443; b) H. Wei, Q. Zhang, Y. Yao, L. Liu, Y. Liu, J. Leng, *ACS Appl. Mater. Interfaces* **2017**, *9*, 876.
- [3] a) S. Sundaram, D. S. Kim, M. A. Baldo, R. C. Hayward, W. Matusik, *ACS Appl. Mater. Interfaces* **2017**, *9*, 32290; b) B. Q. Y. Chan, Y. T. Chong, S. Wang, C. J. Lee, C. Owh, F. Wang, F. Wang, *Chem. Eng. J.* **2022**, *430*, 132513.
- [4] Q. Ge, A. H. Sakhaei, H. Lee, C. K. Dunn, N. X. Fang, M. L. Dunn, *Sci. Rep.* **2016**, *6*, 31110.
- [5] D. Kokkinis, M. Schaffner, A. R. Studart, *Nat. Commun.* **2015**, *6*, 8643.
- [6] a) A. Samanta, W. Huang, H. Chaudhry, Q. Wang, S. K. Shaw, H. Ding, *ACS Appl. Mater. Interfaces* **2020**, *12*, 18032; b) L. Zhong, H. Zhu, Y. Wu, Z. Guo, *J. Colloid Interface Sci.* **2018**, *525*, 234;
- [7] a) L. Pocivavsek, S. -H. Ye, J. Pugar, E. Tzeng, E. Cerda, S. Velankar, W. R. Wagner, *Biomaterials* **2019**, *192*, 226; b) J. -N. Wang, Y. -Q. Liu, Y. -L. Zhang, J. Feng, H. -B. Sun, *NPG Asia Mater.* **2018**, *10*, e470.
- [8] a) K. Okada, Y. Miura, T. Chiya, Y. Tokudome, M. Takahashi, *RSC Adv.* **2020**, *10*, 28032; b) M. Ebara, K. Uto, N. Idota, J. M. Hoffman, T. Aoyagi, *Adv. Mater.* **2012**, *24*, 273;
- [9] a) S. Bahl, H. Nagar, I. Singh, S. Sehgal, *Mater. Today Proc.* **2020**, *28*, 1302; b) Y. Song, Y. Hu, Y. Zhang, G. Li, D. Wang, Y. Yang, Y. Zhang, Y. Zhang, W. Zhu, J. Li, D. Wu, J. Chu, *ACS Appl. Mater. Interfaces* **2022**, *14*, 37248.
- [10] I. Apsite, S. Salehi, L. Ionov, *Chem. Rev.* **2022**, *122*, 1349.
- [11] a) S. A. Turner, J. Zhou, S. S. Sheiko, V. S. Ashby, *ACS Appl. Mater. Interfaces* **2014**, *6*, 8017; b) X. Luo, H. Lai, Z. Cheng, P. Liu, Y. Li, X. Yu, Y. Liu, *Chem. Eng. J.* **2021**, *403*, 126356.
- [12] a) N. García-Huete, J. M. Cuevas, J. M. Laza, J. L. Vilas, L. M. León, *Polymers* **2015**, *7*, 1674; b) J. Song, M. Gao, C. Zhao, Y. Lu, L. Huang, X. Liu, C. J. Carmalt, X. Deng, I. P. Parkin, *ACS Nano* **2017**, *11*, 9259.

- [13] a) J. K. Park, S. Kim, *Lab Chip* **2017**, *17*, 1793; b) Y. Shao, J. Zhao, Y. Fan, Z. Wan, L. Lu, Z. Zhang, W. Ming, L. Ren, *Chem. Eng. J.* **2020**, *382*, 122989.
- [14] a) H. Yang, W. R. Leow, T. Wang, J. Wang, J. Yu, K. He, D. Qi, C. Wan, X. Chen, *Adv. Mater.* **2017**, *29*, 1701627; b) W. Wang, D. Shen, X. Li, Y. Yao, J. Lin, A. Wang, J. Yu, Z. L. Wang, S. W. Hong, Z. Lin, S. Lin, *Angew. Chem. Int. Ed.* **2018**, *57*, 2139.
- [15] J. T. Schiphorst, Technische Universiteit Eindhoven, Eindhoven, Netherlands **2018**.
- [16] D. Habault, H. Zhang, Y. Zhao, *Chem. Soc. Rev.* **2013**, *42*, 7244.
- [17] G. Stoychev, A. Kirillova, L. Ionov, *Adv. Opt. Mater.* **2019**, *7*, 1900067.
- [18] M. Herath, J. Epaarachchi, M. Islam, C. Yan, F. Zhang, J. Leng, *J. Intell. Mater. Syst. Struct.* **2019**, *30*, 3124.
- [19] S. Xu, X. Bai, L. Wang, *Inorg. Chem. Front.* **2018**, *5*, 751.
- [20] A. Raza, U. Hayat, T. Rasheed, M. Bilal, H. M. N. Iqbal, *J. Mater. Res. Technol.* **2019**, *8*, 1497.
- [21] X. Lin, W. Xie, Q. Lin, Y. Cai, Y. Hua, J. Lin, G. He, J. Chen, *Polym. Chem.* **2021**, *12*, 3375.
- [22] Z.-Z. Jiao, H. Zhou, X.-C. Han, D.-D. Han, Y.-L. Zhang, *J. Colloid Interface Sci.* **2023**, *629*, 582.
- [23] G. Constante, I. Apsite, P. Auerbach, S. Aland, D. Schönfeld, T. Pretsch, P. Milkin, L. Ionov, *ACS Appl. Mater. Interfaces* **2022**, *14*, 20208.
- [24] P. Milkin, M. Danzer, L. Ionov, *Macromol. Rapid Commun.* **2022**, *43*, 2200307.
- [25] C. Py, P. Reverdy, L. Doppler, J. Bico, B. Roman, C. N. Baroud, *Phys. Rev. Lett.* **2007**, *98*, 156103.
- [26] H. Brooks, C. Wright, S. Harris, A. Fsadni, *Addit. Manuf.* **2018**, *22*, 138.